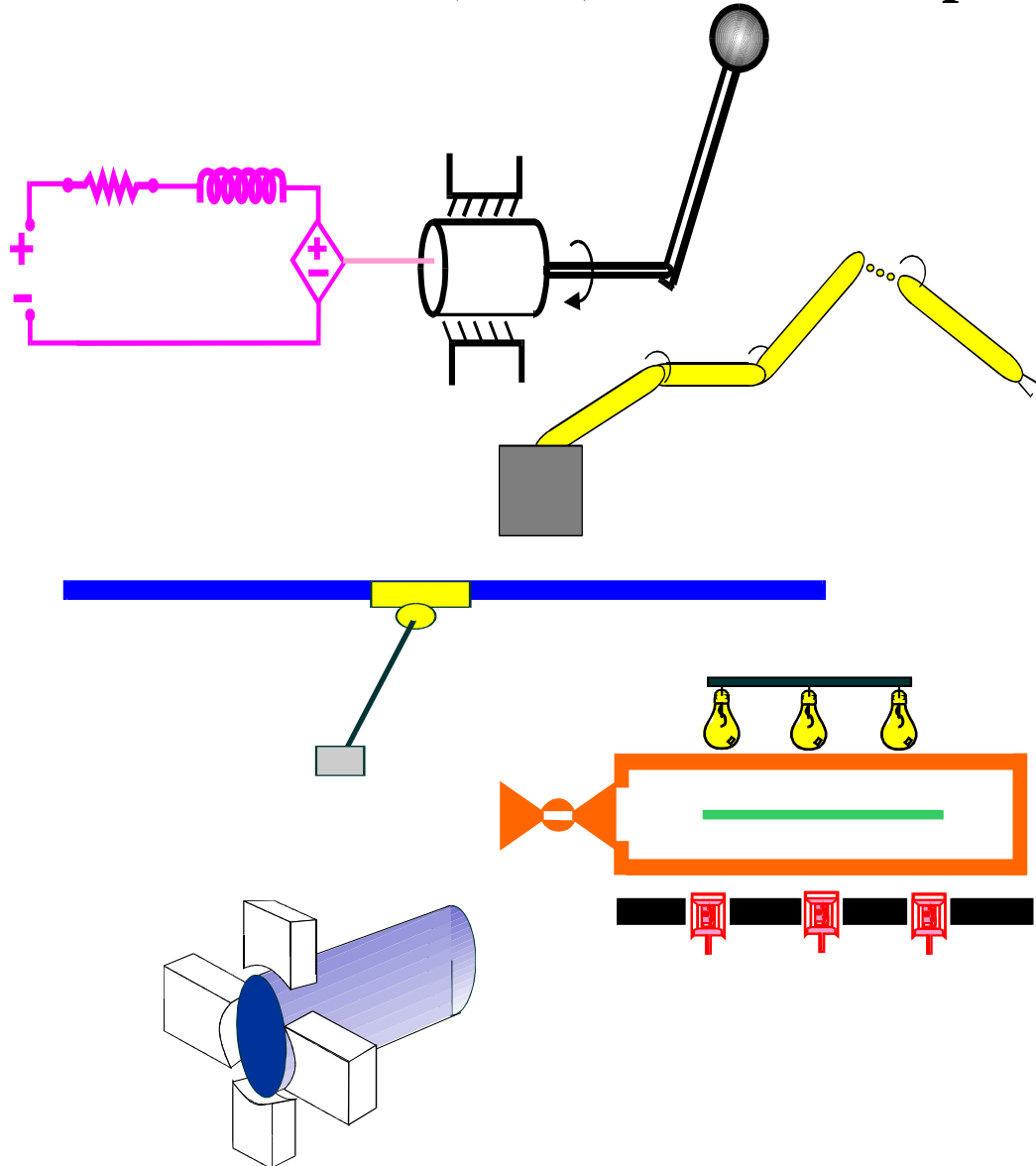


Clemson University
College of Engineering and Science
Control and Robotics (CRB) Technical Report



Number: CU/CRB/09/23/09/#2

Title: Rotor Velocity Control and Efficiency Optimization
of an Induction Motor Driving an Uncertain Load

Authors: Erhun Iyasere, Michael L. McIntyre, Enver
Tatlicioglu, and Darren M. Dawson

Rotor Velocity Control and Efficiency Optimization of an Induction Motor Driving an Uncertain Load

Erhun Iyasere*, Michael L. McIntyre, Enver Tatlicioğlu, and Darren M. Dawson

Abstract—An adaptive controller is presented for an induction motor which yields simultaneous asymptotic rotor velocity/flux tracking without requiring rotor flux measurements and in the presence of uncertainty in the mechanical subsystem parameters. For the rotor flux control problem, it is shown that the desired rotor flux magnitude is generated to minimize the copper loss, hence maximizing energy efficiency in the induction machine. As the mechanical subsystem parameters are uncertain, an optimization algorithm is designed to iteratively seek the optimum rotor flux magnitude that minimizes the induction motor copper loss. Simulation results are presented to illustrate the performance of the control structure.

Index Terms— Adaptive control, Induction motors, Lyapunov methods, Optimization methods

I. INTRODUCTION

The induction motor is the preferred choice of actuator in most industrial applications owing to its simple and rugged construction, absence of brushes, and low cost. Some of these advantageous characteristics create inherent difficulty in controlling the mechanical characteristics of the motor (like rotor position and speed) due to the complexities associated with the relationship between these mechanical characteristics and the applied stator voltage which is commonly used as the control input. Therefore, the utilization of the induction motor in demanding applications (i.e. position tracking, flux tracking, and speed tracking) requires the development of nonlinear control strategies to overcome problems due to: (i) nonlinear coupling in the form of bilinear terms composed of the stator electrical current, rotor flux and rotor velocity, (ii) the impracticality of using full state feedback in control applications as the rotor flux measurements are usually not available, and (iii) uncertainty in motor parameters (e.g. susceptibility of the rotor resistance to temperature). To deal with these difficulties, researchers have proposed various

control strategies for induction motors. One common industrial approach involves approximating the electromechanical dynamics by assuming that the motor speed is statically related to the frequency of the applied voltage and subsequently controlling the motor speed using variable frequency drives (VFDs). One perceived disadvantage of this strategy is the difficulty in improving the efficiency of the induction motor. Some researchers utilized the full-order induction motor model while designing nonlinear control laws. First, assuming all states (including the rotor flux) are measurable, control strategies developed include field oriented control [1]-[3] and input output linearizing control [4]-[6]. However measuring the rotor flux is impractical and nullifies the argument for using the induction motor due to its simplicity of construction, thus several researchers [7]-[22] developed partial-state feedback control strategies to jointly achieve rotor position/velocity tracking by using rotor flux observers or surrogates in order to compensate for the lack of rotor flux measurements. Chang et al. [18] proposed a nonlinear adaptive sensorless speed controller for the induction motor that compensated for parametric uncertainty associated with the rotor resistance. Feemster et al. [19] developed a sensorless (without the presence of any mechanical sensors) rotor velocity tracking controller for induction motors by using a novel rotor velocity observer where the only available measurements were the stator currents. Some of the shortcomings encountered and subsequently remedied by these approaches include: (i) control singularities which occur when the magnitude of the actual or the estimated rotor flux tends to zero, thus resulting in local stability results, (ii) neglecting of the system nonlinearities, and (iii) the tracking error convergence rates being determined by mechanical subsystem parameters as opposed to control gains.

Further constraints imposed by researchers on the induction motor control problem include (parametric) uncertainties present in the dynamic models. Nonlinear adaptive control techniques have been applied when subsystem parameters are unknown. Marino et al. [6] designed a nonlinear adaptive input-output linearizing control strategy for velocity tracking of an induction motor where full-state feedback was available. The load torque and rotor resistance were constant unknown parameters and it was shown that a nonlinear identification

* To whom all correspondence should be addressed. (e-mail: oiyaser@clemson.edu, phone: 864 986 9311)

E. Iyasere and D. M. Dawson are with the Department of Electrical and Computer Engineering, Clemson University, Clemson, SC 29631 USA, M. L. McIntyre, is with the Department of Engineering, Western Kentucky University, Bowling Green, KY 42101, USA.

E. Tatlicioğlu is with the Department of Electrical and Electronics Engineering, Izmir Institute of Technology, Izmir, 35430, Turkey.

scheme could be used to asymptotically identify these unknown values. In [23], Marino et al. designed a global adaptive output feedback rotor speed controller for induction motors where the speed and stator current measurements were the only available measurements and the torque load and rotor resistance were assumed to be constant and unknown. Similar work was done by Dawson et al. [24], [25] where the proposed controllers compensate for uncertainties in the rotor resistance and all mechanical subsystem parameters.

In addition to the conventional tracking problem, additional research has focused on maximizing the efficiency of induction motors. In the control problem of efficiency optimization, induction motors are used to drive loads at constant speeds while the motor power losses are simultaneously minimized. The various methods proposed by researchers can be classified into two basic types: (i) the computation of the optimum rotor flux *a priori* using a loss model, and (ii) real-time computation of losses and the utilization of a search algorithm to determine the maximum efficiency. Kirschen et al. [26] adaptively adjusted the rotor flux of an induction motor by measuring the input power in order to achieve optimal efficiency while utilizing field oriented control to command the motor torque and speed. Sousa et al. [27] described a fuzzy logic-based on-line efficiency optimization strategy for an induction motor in which an indirect vector controller was utilized. A fuzzy controller is used to adjust the excitation current based on the measured input power such that at a given speed and torque, the measured input power is at its minimum. When the load torque or speed commands change, the optimization search algorithm was abandoned and the rated flux of the induction motor was sought instead. Kiokerdis and Margaritis [28] examined loss minimization of induction motor drives using search controllers. They discovered that problems arise when the input power is used as the controlled variable and proved that better results are achieved when the stator current is used as the controlled variable. Poirer et al. [29] proposed a novel approach to improve the induction motor efficiency by using genetic algorithms. Differing from previously discussed strategies which used input power as the variable to be minimized, this strategy directly minimized a developed induction motor loss model by controlling the magnetizing rotor flux. Researchers have also utilized neural networks as well as flux/torque decoupling to minimize motor losses by adjusting the flux-producing current [30], the stator voltage/frequency [31] and the slip frequency [32]. Vedagarbha et al. [33] developed a singularity-free controller for rotor velocity/rotor flux tracking in the induction motor without requiring the measurement of the rotor flux. By using Lyapunov arguments, they proved that the controller yields global exponential stability. Additionally, they showed how the desired rotor flux magnitude in the rotor velocity/flux setpoint control problem can be selected offline to minimize the copper losses. However in their development, the restrictive exact model assumption was made which assumed exact knowledge of all the system parameters.

This paper illustrates how the results in [33] can be extended to derive a singularity-free rotor velocity/flux tracking controller for an induction motor driving a load with uncertain mechanical subsystem parameters. This constraint of uncertainty in the mechanical subsystem provides improvement over [33] where exact knowledge of system parameters was assumed in the design of the control law. Another focus of the current research is the development of an online efficiency optimization technique that minimizes the induction motor copper losses. To meet these objectives, first, an adaptive controller is developed to achieve rotor velocity and rotor flux tracking, provided that the rotor velocity and stator current measurements are available. The control strategy relies on the astute design of the desired torque trajectory signal which ensures asymptotic tracking of a desired rotor velocity. The bilinear structure of the static torque transmission relationship and the structure of the rotor flux dynamics motivate the design of the desired current and flux trajectories, which ensure that the desired torque is delivered to the electromechanical system, the cancellation of current/flux tracking error interconnection terms between the mechanical and electrical subsystems, and that the “magnitude” of the rotor flux asymptotically tracks a desired auxiliary positive function. The desired stator current trajectory is then used along with the stator current electrical dynamics in the construction of the stator (control) voltage by employing the integrator backstepping technique to ensure asymptotic stator current tracking. Lyapunov-based analysis techniques were utilized to generate the adaptation laws for the parameter estimates and to prove asymptotic rotor velocity, rotor flux and stator current tracking. Finally, to minimize the induction motor copper losses, the desired rotor flux magnitude is generated by an online extremum seeking optimization algorithm. An online algorithm is required due to the unknown motor load and uncertainties in the mechanical subsystem dynamics while in [33] these parameters were known *a priori* (exact model knowledge) which implies that the optimum rotor flux magnitude was also known *a priori*.

The remainder of the paper is organized as follows; Section II describes the electromechanical model. Section III describes the formulation of the control problem and the development of the controller. Section IV describes the development of the copper loss reduction strategy. Numerical simulation results, presented in Section V, validate the performance of the control strategy. Finally, concluding remarks are presented in Section VI.

II. ELECTROMECHANICAL MODEL

Based on the assumptions of equal mutual inductances and a linear magnetic circuit, the electromechanical model of an induction motor actuating a mechanical subsystem in the rotating rotor reference frame can be written as follows [34]

$$M_m \dot{\omega} + B\omega + T_L(\omega) = \tau = \alpha_1 I^T J \psi \quad (1)$$

$$\dot{\psi} = -B_1 \psi + B_2 I \quad (2)$$

$$L_r \dot{I} = B_3 \psi - \alpha_1 \omega J \psi - R_l I - L_l \omega J I + V \quad (3)$$

where $\omega(t) \in \mathbb{R}$ and $\dot{\omega}(t) \in \mathbb{R}$ represent the rotor velocity and acceleration, respectively, $\tau(t) \in \mathbb{R}$ is the electromagnetic torque, $M_m \in \mathbb{R}$ is the mechanical inertia of the system (including the rotor inertia), $B \in \mathbb{R}$ denotes the coefficient of viscous friction, $T_L(\omega) \in \mathbb{R}$ denotes the uncertain nonlinear load, $I(t) = [I_a(t) \ I_b(t)]^T \in \mathbb{R}^2$, $\psi(t) = [\psi_a(t) \ \psi_b(t)]^T \in \mathbb{R}^2$, $V(t) = [V_a(t) \ V_b(t)]^T \in \mathbb{R}^2$, represent the stator current, rotor flux, and stator voltage of the induction motor, respectively. In (1)-(3), $L_l, \alpha_1, B_1, B_2, B_3, R_l \in \mathbb{R}$ are positive constants related to the electric circuit parameters which are explicitly defined as follows:

$$\begin{aligned} L_l &= L_s \left(1 - \frac{M^2}{L_s L_r} \right), \quad R_l = \left(R_s + \frac{R_r M^2}{L_r^2} \right) \\ \alpha_1 &= \frac{n_p M}{L_r}, \quad B_1 = \frac{R_r}{L_r}, \quad B_2 = \frac{R_r M}{L_r}, \quad B_3 = \frac{M R_r}{L_r^2} \end{aligned} \quad (4)$$

where $L_r, L_s, M \in \mathbb{R}$ denote the rotor inductance, stator inductance, and mutual inductance of the motor, respectively, $R_r, R_s \in \mathbb{R}$ represent the rotor resistance and stator resistance, respectively, and $n_p \in \mathbb{R}$ is the number motor pole pairs. In (1) and (3), $J \in \mathbb{R}^{2 \times 2}$ is a skew symmetric matrix defined as follows

$$J = \begin{bmatrix} 0 & -1 \\ 1 & 0 \end{bmatrix}. \quad (5)$$

Assumption 1: The parameters of electrical subsystem $L_l, \alpha_1, B_1, B_2, B_3, R_l$ are assumed to be known constants. The mechanical subsystem parameters are assumed to be unknown while knowledge of upper and lower bounds for the mechanical inertia of the system M_m are required *a priori* (i.e. $\underline{M}_m < M_m < \bar{M}_m$ where \underline{M}_m and \bar{M}_m are known positive constants).

Assumption 2: The nonlinear load $T_L(\omega)$ is linearly parameterizable in the sense that $T_L(\omega) = T_{Lw}(\omega) T_{L0}$ where $T_{Lw}(\omega) \in \mathbb{R}^{1 \times q}$ is a known differentiable regression vector dependent on the rotor velocity and $T_{L0} \in \mathbb{R}^q$ is an unknown constant vector. The terms $T_L(\omega)$ and $\dot{T}_L(\omega, \dot{\omega})$ are bounded provided that $\omega(t)$ and $\dot{\omega}(t)$ are bounded.

III. PROBLEM FORMULATION

The control objective is to track a desired rotor speed

$\omega_d(t) \in \mathbb{R}$, while maximizing the motor efficiency by reducing the induction motor copper loss such that

$$\omega(t) \rightarrow \omega_d(t) \text{ and } P_{\text{loss}} \left(\|\psi(t)\|^2 \right) \rightarrow P_{\text{loss}}^* \text{ as } t \rightarrow \infty \quad (6)$$

where $P_{\text{loss}} \left(\|\psi(t)\|^2 \right) \in \mathbb{R}$ is the induction motor copper loss, that will be defined in Section IV, $\|\cdot\|$ denotes the standard Euclidian norm and $P_{\text{loss}}^* \in \mathbb{R}$ is the minimum copper loss at steady state (constant rotor speed and load torque).

Remark 1: The desired rotor velocity is designed such that $\omega_d(t), \dot{\omega}_d(t), \ddot{\omega}_d(t)$ are bounded and known. Since induction motor efficiency optimization is usually performed at constant rotor speed and torque, the desired velocity will be designed to converge to a constant speed.

To quantify the control objective, the rotor velocity tracking error, denoted by $e(t) \in \mathbb{R}$, is defined as follows

$$e = \omega_d - \omega. \quad (7)$$

To facilitate the control design, a filtered tracking error signal, denoted by $r(t) \in \mathbb{R}$, is defined as follows

$$r = e + k_1 \int_0^t e(\sigma) d\sigma \quad (8)$$

where $k_1 \in \mathbb{R}$ is a constant positive control gain.

Remark 2: Based on the definition of $r(t)$ given in (8), standard linear analysis tools [35] can be used to prove that: (i) if $r(t)$ is bounded, then $e(t)$ is bounded, and (ii) if $r(t)$ is asymptotically regulated, then $e(t)$ is asymptotically regulated.

As mentioned previously, in addition to the rotor speed tracking objective, the secondary objective is to minimize the induction motor copper losses by controlling the rotor flux magnitude. To this end, the rotor flux ‘‘magnitude’’¹ tracking error, denoted by $\eta_\delta(t) \in \mathbb{R}$ is also introduced

$$\eta_\delta = \delta_d^2 - \|\psi\|^2 \quad (9)$$

where $\delta_d(t) \in \mathbb{R}$ denotes the desired rotor flux magnitude.

Remark 3: $\delta_d(t)$ is designed: (i) to be strictly positive, (ii) to reduce the induction motor copper loss by converging to the optimum rotor flux magnitude δ_d^* , and (iii) such that $\delta_d(t), \dot{\delta}_d(t), \ddot{\delta}_d(t)$ are bounded.

In addition, to facilitate the subsequent control

¹ In this paper, the rotor flux magnitude refers to the term $\psi_a^2 + \psi_b^2$, which is actually the square of the rotor flux magnitude in strict mathematical terms.

development, the rotor flux tracking error $\eta_\psi(t) \in \mathbb{R}^2$ and the stator current tracking error $\eta_i(t) \in \mathbb{R}^2$ are defined as follows

$$\eta_\psi = \psi_d - \psi, \quad \eta_i = I_d - I \quad (10)$$

where $\psi_d(t) \in \mathbb{R}^2$ and $I_d(t) \in \mathbb{R}^2$ denote the subsequently designed desired rotor flux and stator current trajectories, respectively.

A. Design of the desired rotor flux and stator current trajectories

The desired rotor flux signal $\psi_d(t)$ is defined as follows

$$\psi_d = \delta_d \begin{bmatrix} \cos \rho_d \\ \sin \rho_d \end{bmatrix} \quad (11)$$

where $\rho_d(t) \in \mathbb{R}$ denotes an auxiliary signal that will be designed subsequently. It should be noted that, based on Remark 3, it can be inferred that $\psi_d(t) \in \mathcal{L}_\infty^2$.

The desired stator current $I_d(t)$ is defined as follows:

$$I_d = \begin{bmatrix} \cos \rho_d & -\sin \rho_d \\ \sin \rho_d & \cos \rho_d \end{bmatrix} \begin{bmatrix} I_{d1} \\ I_{d2} \end{bmatrix} \quad (12)$$

where $I_{d1}(t) \in \mathbb{R}$ and $I_{d2}(t) \in \mathbb{R}$ are subsequently designed. From (11), $I_d(t)$ can be expressed in terms of $\psi_d(t)$ as follows

$$I_d = I_{d1} \frac{\psi_d}{\delta_d} + I_{d2} J \frac{\psi_d}{\delta_d}. \quad (13)$$

Remark 4: Based on the structure of (11), the following relationship can be determined

$$\|\psi_d\|^2 = \delta_d^2. \quad (14)$$

Given (14), the rotor flux magnitude tracking error introduced in (9) can be re-written as follows

$$\eta_\delta = \|\psi_d\|^2 - \|\psi\|^2 = (\psi_d + \psi)^T \eta_\psi \quad (15)$$

where $\eta_\psi(t) \in \mathbb{R}^2$ was previously defined in (10). In the subsequent sections, it will be shown that if $\eta_\psi(t)$ is asymptotically stable and if $\psi_d(t), \psi(t) \in \mathcal{L}_\infty$, then $\eta_\delta(t)$ is asymptotically stable. Hence, the secondary objective defined in (9) will be achieved if said conditions are met.

B. Velocity tracking error system

By taking the time derivative of velocity tracking error in (8), then multiplying the resulting expression by M_m , and substituting the mechanical subsystem dynamics in (1), the following expression is obtained

$$M_m \dot{r} = M_m (\dot{\omega}_d + k_1 e) + W_m \theta_m - \alpha_1 I^T J \psi, \quad (16)$$

where $W_m(\omega) = [\omega \quad T_{LW}(\omega)] \in \mathbb{R}^{1 \times p}$ is a measurable regression vector, $\theta_m = [B \quad T_{L\theta}]^T \in \mathbb{R}^p$ is a vector of unknown constants and $p = q + 1$. To facilitate the subsequent design steps, the desired torque signal denoted by $\tau_d(t) \in \mathbb{R}$ is defined as

$$\tau_d = \alpha_1 I_d^T J \psi_d. \quad (17)$$

Remark 5: To ensure the equality of (17), the desired stator current component, $I_{d2}(t)$ in (13), is designed to be

$$I_{d2} = \frac{\tau_d}{\alpha_1 \delta_d}. \quad (18)$$

After adding and subtracting (17) to the right hand side of (16) and then utilizing the current and flux tracking errors given in (10), the expression in (16) can be rewritten as

$$M_m \dot{r} = M_m (\dot{\omega}_d + k_1 e) + W_m \theta_m - \tau_d + \alpha_1 (I_d^T J \eta_\psi + \eta_i^T J \psi_d - \eta_i^T J \eta_\psi). \quad (19)$$

Based on the structure of (19), the desired torque signal is designed to be

$$\tau_d = \hat{M}_m (\dot{\omega}_d + k_1 e) + W_m \hat{\theta}_m + k_s r, \quad (20)$$

where $k_s \in \mathbb{R}^+$ is a constant control gain, and $\hat{M}_m(t) \in \mathbb{R}$, $\hat{\theta}_m(t) \in \mathbb{R}^p$ denote the estimates of M_m and θ_m , respectively, whose update laws are designed subsequently. After substituting (20) into (19), the following closed-loop error system is obtained for $r(t)$

$$\begin{aligned} M_m \dot{r} = & \tilde{M}_m (\dot{\omega}_d + k_1 e) + W_m(\cdot) \tilde{\theta}_m \\ & + \alpha_1 (\eta_i^T J \psi_d + I_d^T J \eta_\psi - \eta_i^T J \eta_\psi) - k_s r \end{aligned} \quad (21)$$

where $\tilde{M}_m(t) \in \mathbb{R}$, $\tilde{\theta}_m(t) \in \mathbb{R}^p$ are estimation errors defined as follows

$$\tilde{M}_m = M_m - \hat{M}_m \quad \tilde{\theta}_m = \theta_m - \hat{\theta}_m. \quad (22)$$

C. Rotor flux tracking error system and desired stator current design

Taking the time derivative of the rotor flux tracking error, $\eta_\psi(t)$ defined in (10) and substituting the rotor flux dynamics in (2), yields the following open-loop rotor flux tracking error system

$$\dot{\eta}_\psi = \dot{\psi}_d + B_1\psi - B_2I. \quad (23)$$

After utilizing the stator current and rotor flux tracking errors defined in (10), the open-loop tracking rotor flux error dynamics can be rewritten as

$$\dot{\eta}_\psi = \dot{\psi}_d + B_1\psi_d - B_1\eta_\psi - B_2I_d + B_2\eta_I. \quad (24)$$

After substituting the time derivative of the desired rotor flux trajectory $\psi_d(t)$ defined in (11), the open-loop error system can be expressed as

$$\dot{\eta}_\psi = \dot{\delta}_d \begin{bmatrix} \cos \rho_d \\ \sin \rho_d \end{bmatrix} + \dot{\rho}_d \delta_d \begin{bmatrix} -\sin \rho_d \\ \cos \rho_d \end{bmatrix} + B_1\psi_d - B_1\eta_\psi - B_2I_d + B_2\eta_I. \quad (25)$$

Using the definition of $\psi_d(t)$ in (11), the rotor flux tracking error dynamics can be rewritten as

$$\dot{\eta}_\psi = \dot{\delta}_d \frac{\psi_d}{\delta_d} + \dot{\rho}_d J\psi_d + B_1\psi_d - B_1\eta_\psi - B_2I_d + B_2\eta_I. \quad (26)$$

Using the definition of the desired stator current $I_d(t)$ in (13) and the current component $I_{d2}(t)$ in (18), the expression in (26) can be rewritten as

$$\dot{\eta}_\psi = \frac{\dot{\delta}_d}{\delta_d} \psi_d + \dot{\rho}_d J\psi_d + B_1\psi_d - B_1\eta_\psi - B_2 \left(\frac{I_{d1}}{\delta_d} \psi_d + \frac{\tau_d}{\alpha_1 \delta_d^2} J\psi_d \right) + B_2\eta_I. \quad (27)$$

Based on the structure of (27), the desired stator current component $I_{d1}(t)$ and $\dot{\rho}_d(t)$ are designed as follows

$$I_{d1} = \frac{B_1}{B_2} \delta_d + \frac{\dot{\delta}_d}{B_2} + \frac{\tau_d r}{B_2 \delta_d} \quad (28)$$

$$\dot{\rho}_d = \frac{B_2 \tau_d}{\alpha_1 \delta_d^2} + \alpha_1 r \left(\frac{B_1}{B_2} + \frac{\delta_d}{B_2 \delta_d} + \frac{\tau_d r}{B_2 \delta_d^2} \right). \quad (29)$$

Substituting (28) and (29) into (27) results in the following closed loop error system for $\eta_\psi(t)$

$$\dot{\eta}_\psi = -B_1\eta_\psi + B_2\eta_I + \alpha_1 r J I_d. \quad (30)$$

Substituting (18) and (28) into (13) results the following expression for the desired stator current trajectory

$$I_d = \frac{\tau_d}{\alpha_1 \delta_d^2} J\psi_d + u_f \psi_d \quad (31)$$

where $u_f(t) \in \mathbb{R}$ is defined as follows

$$u_f = \frac{B_1}{B_2} + \frac{\dot{\delta}_d}{\delta_d B_2} + \frac{\tau_d r}{B_2 \delta_d^2}. \quad (32)$$

D. Stator current tracking error system

The final step in the design procedure is the design of the stator voltage $V(t)$ to ensure that the stator current tracking error, $\eta_I(t)$ defined in (10) tend to zero. Taking the time derivative of the stator current tracking error, and then multiplying by $L_l M_m$ results in the following open-loop error system

$$L_l M_m \dot{\eta}_I = L_l M_m \begin{pmatrix} \frac{\dot{\tau}_d}{\alpha_1 \delta_d^2} J\psi_d - \frac{2\tau_d \dot{\delta}_d}{\alpha_1 \delta_d^3} J\psi_d \\ + \frac{\tau_d}{\alpha_1 \delta_d^2} J\dot{\psi}_d + \dot{u}_f \psi_d + u_f \dot{\psi}_d \end{pmatrix} - M_m \begin{pmatrix} B_3(\psi_d - \eta_\psi) - (R_l + L_l \omega J)I \\ -\alpha_1 \omega J(\psi_d - \eta_\psi) + V \end{pmatrix}. \quad (33)$$

where the current dynamics in (2), (10), and the time derivative of (31) were utilized.

The signals $\dot{\tau}_d(t)$ and $\dot{u}_f(t)$ can be obtained as follows

$$\dot{\tau}_d = \frac{\partial \tau_d}{\partial \hat{M}_m} \dot{\hat{M}}_m + \frac{\partial \tau_d}{\partial \hat{\theta}_m} \dot{\hat{\theta}}_m + \frac{\partial \tau_d}{\partial q} \omega + \frac{\partial \tau_d}{\partial \omega} \dot{\omega} + \frac{\partial \tau_d}{\partial t} \quad (34)$$

$$\dot{u}_f = \frac{\partial u_f}{\partial t} + \frac{\partial u_f}{\partial \hat{M}_m} \dot{\hat{M}}_m + \frac{\partial u_f}{\partial \hat{\theta}_m} \dot{\hat{\theta}}_m + \frac{\partial u_f}{\partial q} \omega + \frac{\partial u_f}{\partial \omega} \dot{\omega} + \frac{\partial u_f}{\partial \delta_d} \dot{\delta}_d + \frac{\partial u_f}{\partial \dot{\delta}_d} \ddot{\delta}_d \quad (35)$$

where (20) and (32) were utilized, $q(t) \triangleq \int_0^t \omega(\sigma) d(\sigma) \in \mathbb{R}$ denotes the rotor position, and the partial derivative terms are defined in Appendix I. Except for the rotor acceleration, $\dot{\omega}(t)$, all the remaining terms on the right hand sides of (34) and (35) are measurable including the subsequently designed $\dot{\hat{M}}_m(t)$ and $\dot{\hat{\theta}}_m(t)$. After utilizing (1) and (10), the rotor acceleration can be expressed as follows

$$\dot{\omega}(t) = \frac{(\alpha_1 I^T J (\psi_d - \eta_\psi) - W_m \theta_m)}{M_m} \quad (36)$$

where $W_m(\cdot)$ and θ_m were previously introduced in (16). After substituting (34), (35) and (36) into (33) and carefully grouping terms, the open-loop stator current tracking error system can be expressed as

$$L_l M_m \dot{\eta}_l = \Omega_a + M_m \Omega_b + Y \theta_m + \Omega_c \eta_\psi + M_m \Omega_d \eta_\psi + M_m B_3 \eta_\psi - M_m V \quad (37)$$

where $Y(t) \in \mathbb{R}^{2 \times p}$, $\Omega_a, \Omega_b \in \mathbb{R}^2$ and $\Omega_c, \Omega_d \in \mathbb{R}^{2 \times 2}$ denote measurable auxiliary functions defined in Appendix II. Based on the structure of (21), (30) and (37) and the subsequent stability analysis motivates the following design of the voltage control input

$$V = k_e \eta_l + \Omega_b + \frac{1}{\hat{M}_m} (\Omega_a + Y \hat{\theta}_m + \alpha_1 r J \psi_d) + k_n \|\Omega_c\|_\infty^2 \eta_l + k_n \|\Omega_d\|_\infty^2 \eta_l + k_n \alpha_1^2 r^2 \eta_l + k_n (B_2 + B_3)^2 \eta_l \quad (38)$$

where $k_e \in \mathbb{R}^+$ is a constant control gain, $k_n \in \mathbb{R}^+$ is a damping constant and $\|\cdot\|_\infty$ denotes the infinity norm. After substituting (38) into (37) and using the definitions of the parameter estimate errors in (22), the following closed-loop stator current tracking error system is obtained

$$L_l M_m \dot{\eta}_l = -k_e M_m \eta_l + Y \tilde{\theta}_m - \alpha_1 r J \psi_d + \left[\Omega_c \eta_\psi - k_n M_m \|\Omega_c\|_\infty^2 \eta_l \right] + M_m \left[\Omega_d \eta_\psi - k_n \|\Omega_d\|_\infty^2 \eta_l \right] + M_m \left[B_3 \eta_\psi - k_n B_3^2 \eta_l \right] - \tilde{M}_m \left[\Omega_a + Y \theta_m + \alpha_1 r J \psi_d \right] \hat{M}_m^{-1} - k_n M_m (\alpha_1^2 r^2 + B_2^2) \eta_l \quad (39)$$

E. Development of parameter update law

Based on the subsequent stability analysis, the update law $\dot{\hat{\theta}}_m(t) \in \mathbb{R}^p$ is designed as

$$\dot{\hat{\theta}}_m = \Gamma_1 (W_m^T r + Y^T \eta_l). \quad (40)$$

where $\Gamma_1 \in \mathbb{R}^{p \times p}$ is a positive-definite, diagonal gain matrix. The estimator $\hat{M}_m(t) \in \mathbb{R}$ is designed with a projection strategy as follows

$$\dot{\hat{M}}_m = \text{Proj}\{\Omega_m\} \quad (41)$$

$$\Omega_m = \Gamma_2 \left((\dot{\omega}_d + k_1 e) r - \frac{\eta_l^T}{\hat{M}_m} (\Omega_a + Y \hat{\theta}_m + \alpha_1 r J \psi_d) \right). \quad (42)$$

where $\Gamma_2 \in \mathbb{R}^+$ is a constant gain. The projection strategy $\text{Proj}\{\cdot\}$ in (41) ensures that $\hat{M}_m \in [\underline{M}_m, \bar{M}_m]$ as follows

$$\dot{\hat{M}}_m = \begin{cases} \Omega_m & \text{if } \bar{M}_m > M_m > \underline{M}_m \\ \Omega_m & \text{if } M_m = \underline{M}_m \text{ and } \Omega_m \geq 0 \\ \Omega_m & \text{if } M_m = \bar{M}_m \text{ and } \Omega_m \leq 0 \\ 0 & \text{otherwise} \end{cases} \quad (43)$$

F. Composite stability analysis

Theorem 1: The proposed voltage control input in (38), ensures asymptotic rotor velocity/rotor flux tracking in the sense that $e(t), \|\eta_\psi(t)\| \rightarrow 0$ as $t \rightarrow \infty$ provided that the control gain introduced in (38) satisfies the following sufficient condition

$$k_n > \frac{1}{B_1} \left(\frac{3}{\underline{M}_m} + 2\bar{M}_m \right). \quad (44)$$

Proof: To facilitate the proof, a nonnegative Lyapunov function $V_1(t) \in \mathbb{R}$ is defined as follows

$$V_1 = \frac{1}{2} M_m r^2 + \frac{1}{2} \eta_\psi^T \eta_\psi + \frac{1}{2} L_l \eta_l^T \eta_l + \frac{1}{2} \Gamma_1^{-1} \tilde{M}_m^2 + \frac{1}{2} \tilde{\theta}_m^T \Gamma_2^{-1} \tilde{\theta}_m. \quad (45)$$

The non-negative function $V_1(t)$ can be bounded using the Raleigh inequality as follows:

$$\lambda_1 \|z\|^2 \leq V_1 \leq \lambda_2 \|z\|^2 \quad (46)$$

where λ_1 and λ_2 are positive scalars defined as follows:

$$\lambda_1 = \frac{1}{2} \min \left\{ 1, M_m, L_l M_m, \Gamma_1^{-1}, \lambda_{\min} \left\{ \Gamma_2^{-1} \right\} \right\} \\ \lambda_2 = \frac{1}{2} \max \left\{ 1, M_m, L_l M_m, \Gamma_1^{-1}, \lambda_{\max} \left\{ \Gamma_2^{-1} \right\} \right\} \quad (47)$$

and $\lambda_{\min}\{\cdot\}$ and $\lambda_{\max}\{\cdot\}$ denote the minimum and maximum eigenvalues, respectively, and $z(t) \in \mathbb{R}^{6+p}$ is defined as

$$z = \begin{bmatrix} r & \eta_\psi^T & \eta_l^T & \tilde{M}_m & \tilde{\theta}_m^T \end{bmatrix}. \quad (48)$$

Taking the time-derivative of (45) yields the following expression

$$\begin{aligned} \dot{V}_1 = & rM_m \dot{r} + \eta_\psi^T \dot{\eta}_\psi + \eta_I^T L_1 M_m \dot{\eta}_I \\ & + \tilde{\theta}_m^T \Gamma_1^{-1} \dot{\tilde{\theta}}_m + \tilde{M}_m \Gamma_2^{-1} \dot{\tilde{M}}_m. \end{aligned} \quad (49)$$

After substituting the closed loop error systems in (21), (30), and (39), the update laws in (40) and (41), the estimation errors in (22), and then canceling common terms, $\dot{V}_1(t)$ can be arranged in the following advantageous manner:

$$\begin{aligned} \dot{V}_1 = & -k_s r^2 - k_e M_m \|\eta_I\|^2 - B_1 \|\eta_\psi\|^2 \\ & + \left[\eta_I^T \Omega_c \eta_\psi - k_n M_m \|\Omega_c\|_\infty^2 \|\eta_I\|^2 \right] \\ & + M_m \left[\eta_I^T \Omega_d \eta_\psi - k_n \|\Omega_d\|_\infty^2 \|\eta_I\|^2 \right] \\ & + \left[\alpha_1 r \eta_I^T J \eta_\psi - k_n M_m \alpha_1^2 r^2 \|\eta_I\|^2 \right] \\ & + \left[B_2 \eta_\psi^T \eta_I - k_n M_m B_2^2 \|\eta_I\|^2 \right] \\ & + \tilde{M}_m \left(-\frac{\eta_I^T}{\hat{M}_m} (\Omega_a + Y \theta_m + \alpha_1 r J \psi_d) \right. \\ & \left. + (\dot{\omega}_d + k_1 e) r - \Gamma_1^{-1} \text{Proj}\{\Omega_m\} \right). \end{aligned} \quad (50)$$

It should be noted that an adaptive law with the projection algorithm defined on a convex set retains all the properties of the adaptive law without the projection algorithm [36]. Thus, the expression given in (50) can be re-written as follows

$$\begin{aligned} \dot{V}_1 = & -k_s r^2 - k_e M_m \|\eta_I\|^2 - B_1 \|\eta_\psi\|^2 \\ & + \left[\eta_I^T \Omega_c \eta_\psi - k_n M_m \|\Omega_c\|_\infty^2 \|\eta_I\|^2 \right] \\ & + M_m \left[\eta_I^T \Omega_d \eta_\psi - k_n \|\Omega_d\|_\infty^2 \|\eta_I\|^2 \right] \\ & + \left[\alpha_1 r \eta_I^T J \eta_\psi - k_n M_m \alpha_1^2 r^2 \|\eta_I\|^2 \right] \\ & + \left[B_2 \eta_\psi^T \eta_I - k_n M_m B_2^2 \|\eta_I\|^2 \right] \\ & + \tilde{M}_m \left(-\frac{\eta_I^T}{\hat{M}_m} (\Omega_a + Y \theta_m + \alpha_1 r J \psi_d) \right. \\ & \left. + (\dot{\omega}_d + k_1 e) r - \Gamma_1^{-1} \Omega_m \right). \end{aligned} \quad (51)$$

After substituting (42) into (51) and using the nonlinear damping argument [37] on the hard-bracketed terms in (51), the following upper bound on $\dot{V}_1(t)$ is obtained

$$\begin{aligned} \dot{V}_1 \leq & -k_s r^2 - k_e M_m \|\eta_I\|^2 \\ & - B_1 \|\eta_\psi\|^2 + \frac{1}{k_n} \left(\frac{3}{\underline{M}_m} + 2\bar{M}_m \right) \|\eta_\psi\|^2. \end{aligned} \quad (52)$$

From (52), $\dot{V}_1(t)$ can be upper bounded as follows

$$\dot{V}_1 \leq -\lambda_3 \|x\|^2 \quad (53)$$

where $\lambda_3 \in \mathbb{R}$ is a positive constant provided the sufficient condition in (44) holds and is defined by

$$\lambda_3 = \min \left\{ k_s, k_e M_m, \left(B_1 - \frac{1}{k_n} \left(\frac{3}{\underline{M}_m} + 2\bar{M}_m \right) \right) \right\}. \quad (54)$$

and $x(t) \in \mathbb{R}^5$ is defined by

$$x = \begin{bmatrix} r & \eta_I^T & \eta_\psi^T \end{bmatrix}. \quad (55)$$

After integrating (53), the following inequality can be obtained

$$\lambda_3 \int_{t_0}^{\infty} \|x(\sigma)\|^2 d\sigma < V_1(t_0) - V_1(\infty). \quad (56)$$

From (46) and (53), it can be concluded that $V_1(t) \in \mathcal{L}_\infty$ hence $z(t) \in \mathcal{L}_\infty$, $r(t) \in \mathcal{L}_\infty$, $\eta_I(t) \in \mathcal{L}_\infty$, $\eta_\psi(t) \in \mathcal{L}_\infty$, $\tilde{M}_m(t) \in \mathcal{L}_\infty$, $\tilde{\theta}_m(t) \in \mathcal{L}_\infty$ thus $x(t) \in \mathcal{L}_\infty$. Since $r(t) \in \mathcal{L}_\infty$, from Remark 2, it can be concluded that $e(t), \int_0^t e(\sigma) d\sigma \in \mathcal{L}_\infty$ and Remark 1 can be utilized to show that $\omega(t) \in \mathcal{L}_\infty$. Since $\tilde{M}_m(t) \in \mathcal{L}_\infty$, $\tilde{\theta}_m(t) \in \mathcal{L}_\infty$, then from (22), it is easy to see that $\hat{M}_m(t) \in \mathcal{L}_\infty$ and $\hat{\theta}_m(t) \in \mathcal{L}_\infty$. From (56), it is clear that $x(t) \in \mathcal{L}_2$. Given that $\omega(t) \in \mathcal{L}_\infty$, from Assumption 2, it can be concluded that $W_m(\omega) \in \mathcal{L}_\infty$. The expression in (20) can be used along with Remark 1 and the above boundedness statements to show that $\tau_d(t) \in \mathcal{L}_\infty$. Given that $\tau_d(t), r(t) \in \mathcal{L}_\infty$ and Remark 3, it can be inferred from (29) and (32) that $\dot{\rho}_d(t), u_f(t) \in \mathcal{L}_\infty$, respectively, thus from the time-derivative of (11), it is clear that $\dot{\psi}_d(t) \in \mathcal{L}_\infty$. Given that $\tau_d(t), u_f(t) \in \mathcal{L}_\infty$, $\psi_d(t) \in \mathcal{L}_\infty$, from (31) and Remark 3, it can be concluded that $I_d(t) \in \mathcal{L}_\infty$. Given that $z(t) \in \mathcal{L}_\infty$ and $I_d(t), \psi_d(t) \in \mathcal{L}_\infty$, it is clear from (10) that $I(t), \psi(t) \in \mathcal{L}_\infty$. Given the above boundedness statements, it can be inferred that the adaptive estimates $\hat{\theta}_m(t), \hat{M}_m(t)$ designed in (40) and (43) respectively are bounded. This conclusion, in addition to the all previous boundedness statements infers from (38) that $V(t) \in \mathcal{L}_\infty$. It can be concluded that all of the system signals remain bounded during closed-loop operation. Using the closed-loop error systems in (21), (30) and (39); and the above boundedness statements, it can be concluded that $\dot{x}(t) \in \mathcal{L}_\infty$. Since $x(t) \in \mathcal{L}_2 \cap \mathcal{L}_\infty$ and $\dot{x}(t) \in \mathcal{L}_\infty$, Barbalat's lemma [36]

can be invoked to show that $\|x(t)\| \rightarrow 0$ as $t \rightarrow \infty$; thus $r(t), \|\eta_\psi(t)\| \rightarrow 0$ as $t \rightarrow \infty$. From Remark 2, it can be concluded that $e(t) \rightarrow 0$ as $t \rightarrow \infty$.

Theorem 2: The rotor flux magnitude tracking error is asymptotically stable in the sense that $\eta_\delta(t) \rightarrow 0$ as $t \rightarrow \infty$ provided that $\eta_\psi(t)$ is asymptotically stable and $\psi_d(t), \psi(t) \in \mathcal{L}_\infty$.

Proof: Given that $\psi_d(t), \psi(t), \eta_\psi(t) \in \mathcal{L}_\infty$ (see proof of Theorem 1, it is clear from (15) that $\eta_\delta(t) \in \mathcal{L}_\infty$. Given that $\psi(t), I(t) \in \mathcal{L}_\infty$ (see the proof of Theorem 1), from (2), it can be concluded that $\dot{\psi}(t) \in \mathcal{L}_\infty$. The time derivative of (15) can be utilized along with the facts that $\dot{\psi}(t) \in \mathcal{L}_\infty, \dot{\psi}_d(t) \in \mathcal{L}_\infty, \dot{x}(t) \in \mathcal{L}_\infty, \dot{\eta}_\psi(t) \in \mathcal{L}_\infty$ to prove that $\dot{\eta}_\delta(t) \in \mathcal{L}_\infty$. Since the product of an \mathcal{L}_∞ bounded function with an \mathcal{L}_2 bounded function is an \mathcal{L}_2 bounded function, from (15) it can be inferred that $\eta_\delta(t) \in \mathcal{L}_2$. Thus, $\eta_\delta(t) \in \mathcal{L}_2 \cap \mathcal{L}_\infty$ and $\dot{\eta}_\delta(t) \in \mathcal{L}_\infty$, and Barbalat's lemma can be invoked to show that $\eta_\delta(t) \rightarrow 0$ as $t \rightarrow \infty$.

IV. OPTIMUM REDUCTION OF COPPER LOSSES

In many applications, induction motors are required to operate at constant speed. As mentioned previously, in constant speed applications, a secondary objective is to minimize power losses. In this section, an optimum seeking desired trajectory $\delta_d(t)$ is designed to increase the efficiency by minimizing the power (copper) losses during the operation of the induction motor. To facilitate this design, the power loss denoted by $P_{loss}(t)$ is used as the performance index (or cost function) and is given by

$$P_{loss} = V^T I - \tau \omega \quad (57)$$

where the transmitted torque $\tau(t)$ is obtained from (1) as follows

$$\tau = \alpha_1 I^T J \psi. \quad (58)$$

After substituting (3) and (58) for $V(t)$ and $\tau(t)$, respectively into the right hand side of (57), the following power loss relationship for the induction motor is obtained:

$$P_{loss} = L_1 \dot{I}^T I - B_3 \psi^T I + R_f I^T I. \quad (59)$$

Based on the stability analysis from Section III-F, it is clear that at steady state (i.e. after a short transient time), exact

tracking of the desired stator current and desired rotor flux (i.e., $\omega \rightarrow \omega_d, \psi \rightarrow \psi_d$, and $I \rightarrow I_d$) is guaranteed with all time derivatives being equal to zero. Specifically, the desired rotor velocity, rotor flux, and stator current trajectories introduced in (7), (11), and (31), respectively, are substituted into (59) and Remark 4 is used to obtain the following equation

$$P_{loss} = \left(R_s + \frac{M^2}{L_r^2} R_r \right) \frac{L_r^2}{n_p^2 M^2} \frac{\tau_d(\omega_d)^2}{\delta_d^2} + \frac{R_s}{M^2} \delta_d^2. \quad (60)$$

In [33], it was shown that the performance index $P_{loss}(t)$, which is unimodal in terms of δ_d , could be used to obtain the optimum value for $\delta_d(t)$ as

$$\delta_d^* = \sqrt[4]{\left(\frac{L_r^2}{n_p^2} + \frac{R_r M^2}{R_s n_p^2} \right) \tau_d(\omega_d)^2}. \quad (61)$$

In [33], the optimum value was evaluated *a priori* as all the constants in (61) were assumed to be known. In our design, the steady state value of desired torque trajectory $\tau_d(t)$ is not available since the induction motor is driving an uncertain load. Thus, to determine the optimum value for $\delta_d(t)$, differing from [33], an online extremum seeking algorithm must be designed to iteratively seek the value for $\delta_d(t)$ that corresponds to the minimum value of $P_{loss}(t)$. In our design, a gradient descent algorithm is employed which works by taking update steps proportional to the negative of the approximate gradient of the performance index at the current step. The optimization algorithm updates the optimum value $\bar{\delta}_d[n]$ at each iteration step of the optimization algorithm. These updates, $\bar{\delta}_d[n]$, are then passed through a set of second order stable and proper low pass filters to generate continuous and bounded signals for $\delta_d(t), \dot{\delta}_d(t)$ and $\ddot{\delta}_d(t)$. The following filters were utilized

$$\delta_d(t) = \frac{\zeta_3}{\zeta_1 s^2 + \zeta_2 s + \zeta_3} \bar{\delta}_d[n], \quad (62)$$

$$\dot{\delta}_d(t) = \frac{\zeta_3 s}{\zeta_1 s^2 + \zeta_2 s + \zeta_3} \bar{\delta}_d[n], \quad (63)$$

$$\ddot{\delta}_d(t) = \frac{\zeta_3 s^2}{\zeta_1 s^2 + \zeta_2 s + \zeta_3} \bar{\delta}_d[n], \quad (64)$$

where $\zeta_1, \zeta_2, \zeta_3 \in \mathbb{R}$ are positive filter constants, s is the Laplace operator and $n \in \mathbb{Z}^+$ is the iteration step. The optimization algorithm waits between updates until certain criteria are met. In other words, if $|\dot{\omega}_d(t)| \leq \bar{e}_1$,

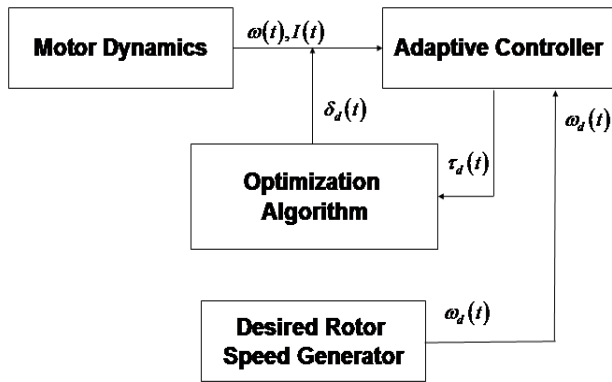


Fig. 1. A block-diagram representation of the developed induction motor efficiency optimization strategy.

$|\bar{\delta}_d[n] - \delta_d(t)| \leq \bar{e}_2$ and $|\omega_d(t) - \omega(t)| \leq \bar{e}_3$, then $n = n + 1$ where $\bar{e}_1, \bar{e}_2, \bar{e}_3 \in \mathbb{R}$ are positive threshold constants. Furthermore the optimization algorithm is assumed to have converged, when the gradient of $P_{loss}(t)$ with respect to $\delta_d(t)$ is within a certain threshold after which the optimization algorithm terminates and stops updating the optimum value $\bar{\delta}_d[n]$. To ensure that $\delta_d(t)$ is strictly positive as stated in Remark 3, the initial value and all subsequent values of $\delta_d(t)$ are restricted to the set $(0, \infty)$.

Based on the design of the optimization algorithm and the preceding stability analysis, it can be concluded that $\|\psi(t)\|^2 \rightarrow \delta_d(t)^2$ as $t \rightarrow \infty$ and $\delta_d(t) \rightarrow \hat{\delta}_d^*$ which implies that $P_{loss}(t) \rightarrow \hat{P}_{loss}^*$, where $\hat{\delta}_d^*$ is the estimated optimum value of $\delta_d(t)$ and \hat{P}_{loss}^* is the estimated minimum of $P_{loss}(t)$, both of which result from the optimization algorithm. From the simulation results in the next section it can be further seen that if $\hat{\delta}_d^* = \delta_d^*$ then $\hat{P}_{loss}^* = P_{loss}^*$ results in the optimal solution. However, if the optimization algorithm does not locate the exact optimal values, then the solution results in a sub-optimal value.

V. SIMULATION RESULTS

A numerical simulation study was conducted to evaluate the induction motor efficiency optimization strategy using MATLAB/Simulink. It should be noted that the adaptive controller developed in Section III and the optimization developed in Section IV were run simultaneously as shown in the flow diagram in Figure 1. All initial values of the rotor velocity, rotor flux and stator current are selected to be zero. The initial conditions of the adaptive update laws given in (40) and (41) are assumed to be $\hat{\theta}_m(t_0) = 0.6\theta_m$ and $\hat{M}_m = 0.6M_m$, respectively. Two cases were considered for simulation: (a) A system with constant unknown load, and (b)

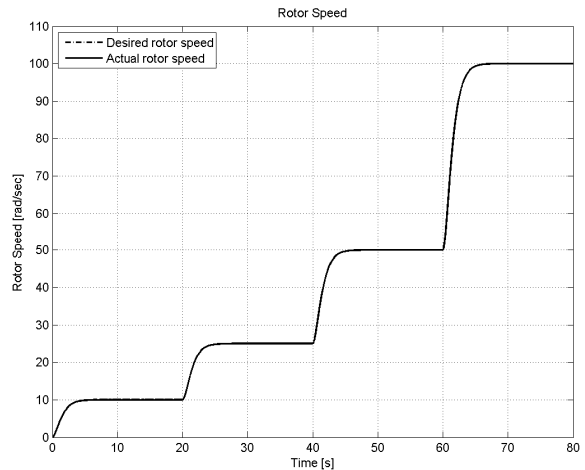


Fig. 2. Desired rotor speed profile $\omega_d(t)$.

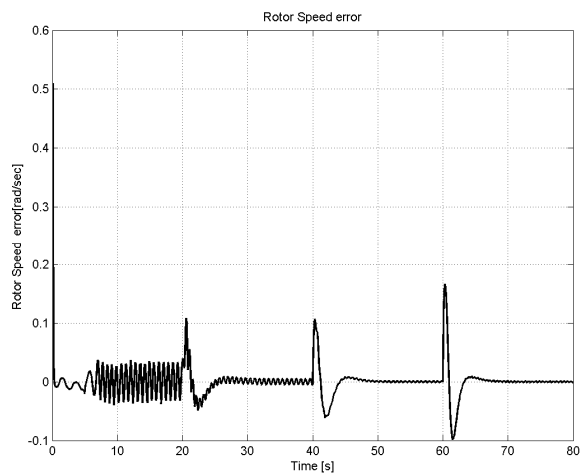


Fig. 3. Rotor speed error $e(t)$ for the constant load case.

A system with an unknown nonlinear load. The following values were used for the system [25], [38]:

$$\begin{aligned} M_m &= 0.044 \text{ [kg} \cdot \text{m}^2] & B &= 0.007 \text{ [kg} \cdot \text{m}^2] \\ R_r &= 1.99 \text{ [}\Omega] & L_r &= 0.14 \text{ [H]} \\ R_s &= 3.2 \text{ [}\Omega] & L_s &= 0.145 \text{ [H]} \\ n_p &= 1 & M &= 0.12 \text{ [H]} \\ \underline{M}_m &= 0.1M_m & \bar{M}_m &= 3M_m & T_{L0} &= 1 \times 10^{-4} \end{aligned}$$

A. System with constant unknown load

In this case, the shaft of the induction motor is assumed to be directly coupled to a device capable of providing a constant load torque of $T_L(\omega) = 0.75 \text{ [Nm]}$ (e.g. a separately excited direct current motor). The desired rotor velocity trajectory, $\omega_d(t)$, was selected to gradually increase from 10 [rad/s] to 100 [rad/s] via a soft start trajectory as shown in Figure 2. This speed profile was chosen to determine whether the efficiency optimization is robust to gradual changes in the desired speed profile. After several test runs, the following

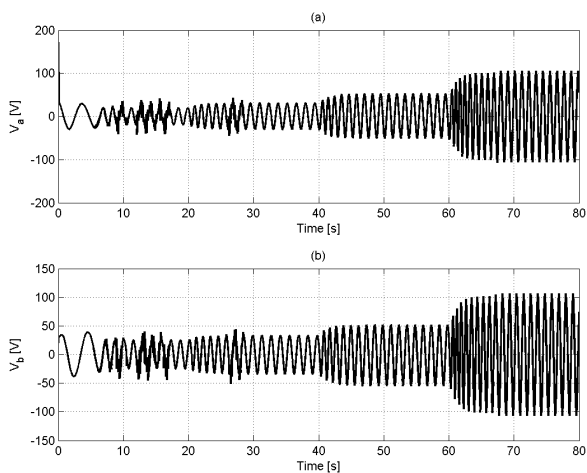


Fig. 4. Time evolution of the control voltage: (a) $V_a(t)$ and (b) $V_b(t)$ for

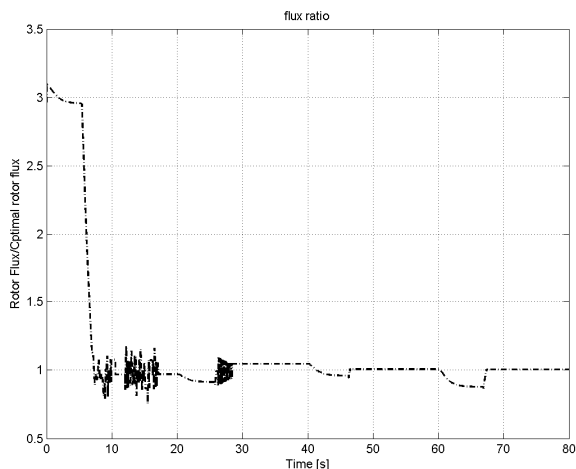


Fig. 5. The time evolution of the rotor magnitude ratio $\frac{\delta_d(t)}{\delta_d^*}$ for the constant load case

control gains were determined to yield the best performance

$$\begin{aligned} k_s=1 \quad k_e=1 \quad k_n=0.1 \quad k_1=1 \\ \Gamma_1 = 1 \times 10^{-3} \quad \Gamma_2 = \text{diag}(1 \times 10^{-3} \quad 1) \end{aligned}$$

The rotor velocity tracking error $e(t)$ is depicted in Figure 3. The control voltage $V(t)$ is shown in Figure 4. The time evolution of the ratio of the designed desired rotor magnitude $\delta_d(t)$ to the optimum value δ_d^* is shown in Figure 5. It can be seen that at steady state, the ratio converges to 1 which implies that $\delta_d(t) \rightarrow \hat{\delta}_d^*$ and $\hat{\delta}_d^* \approx \delta_d^*$. Similarly the time evolution of the ratio of the power $P_{loss}(t)$ to the minimum power loss P_{loss}^* is shown in Figure 6. It can be seen that at steady state, the ratio converges to 1 which implies that $P_{loss}(t) \rightarrow \hat{P}_{loss}^*$ and $\hat{P}_{loss}^* \approx P_{loss}^*$.

B. System with nonlinear unknown load

In this case, the shaft of the induction motor is assumed to be directly coupled to a centrifugal load torque of $T_L(\omega) = T_{Lo} \omega^2$ [Nm]. The desired rotor velocity trajectory, $\omega_d(t)$, is designed to be the same as Case A. After several test runs, the following control gains were determined to yield the best performance

$$\begin{aligned} k_s=1 \quad k_e=1 \quad k_n=0.5 \quad k_1=1 \\ \Gamma_1 = 1 \times 10^{-3} \quad \Gamma_2 = \text{diag}(1 \times 10^{-3} \quad 1 \times 10^{-5}) \end{aligned}$$

The rotor velocity tracking error $e(t)$ is depicted in Figure 7. The control voltage $V(t)$ is shown in Figure 8. The time evolution of the ratio of the designed desired rotor magnitude $\delta_d(t)$ to the optimum value δ_d^* is shown in Figure 9. It can be seen that at steady state, the ratio converges to 1 which implies that $\delta_d(t) \rightarrow \hat{\delta}_d^*$ and $\hat{\delta}_d^* \approx \delta_d^*$. Similarly the time evolution of the ratio of the power $P_{loss}(t)$ to the minimum power loss P_{loss}^* is shown in Figure 10. It can be seen that at steady state, the ratio converges to 1 which implies that $P_{loss}(t) \rightarrow \hat{P}_{loss}^*$ and $\hat{P}_{loss}^* \approx P_{loss}^*$.

Remark 6: The selection of the control parameters in the simulation does not satisfy the condition given in (44) of Theorem 1; however, this requirement is only a sufficient conservative condition generated by the Lyapunov stability argument.

From the simulation results, it can be concluded that the efficiency optimization strategy can effectively reduce the copper loss of an induction motor driving an unknown nonlinear load to a constant speed. Also shown is the robustness of the optimization strategy to changes in the desired rotor speed.

VI. CONCLUSION

A novel approach to improve the efficiency of an induction motor driving an unknown load at a constant speed was presented. The induction motor copper loss was used as the performance index to be minimized. This performance index was shown to be unimodal in terms of the rotor flux magnitude. In the absence of exact model knowledge (unknown load), the optimum rotor flux magnitude is not known *a priori* and an optimization algorithm is presented which seeks the unknown minimum of the performance index by generating a desired rotor flux magnitude trajectory while ensuring that the resulting trajectory remains bounded and sufficiently differentiable. An adaptive controller is then developed to simultaneously track a desired speed profile and the generated rotor flux magnitude trajectory in the presence of unknown mechanical subsystem parameters which results in the minimization of the motor copper losses. It was proven that the developed controller yields asymptotic tracking.

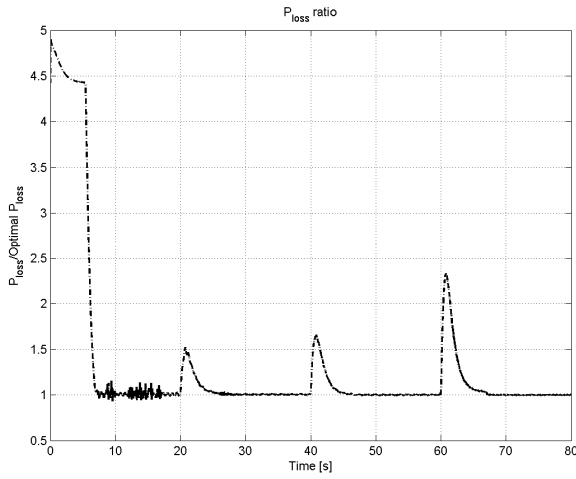


Fig. 6. The time evolution of the copper loss ratio $\frac{P_{loss}(t)}{P_{loss}^*}$ for the constant load case.

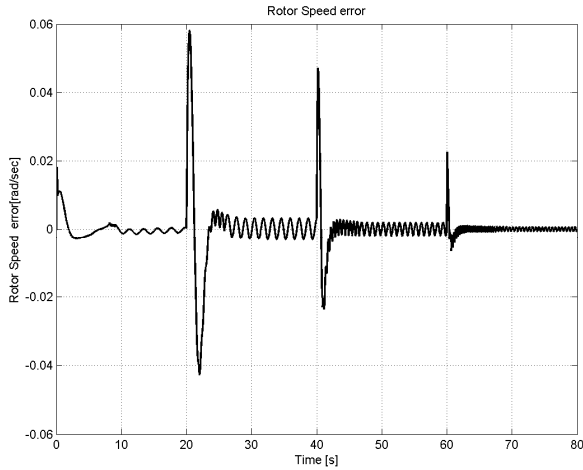


Fig. 7. Rotor speed error $e(t)$ for the nonlinear load case.

Numerical results were presented demonstrating the effectiveness of the control strategy for both constant and varying loads.

APPENDIX I

The partial derivative expression for $\dot{\tau}_d(t)$ and $\dot{u}_f(t)$ are listed as follows:

$$\begin{aligned} \frac{\partial \tau_d}{\partial \hat{M}_m} &= \omega_d + k_1 e, & \frac{\partial \tau_d}{\partial \hat{\theta}_m} &= W_m(\cdot), & \frac{\partial \tau_d}{\partial q} &= -k_s k_1 \\ \frac{\partial \tau_d}{\partial \omega} &= -\hat{M}_m k_1 - k_s + \frac{\partial W_m}{\partial \omega} \hat{\theta}_m \\ \frac{\partial \tau_d}{\partial t} &= \hat{M}_m \ddot{\omega}_d + \hat{M}_m k_1 \dot{\omega}_d + k_s \dot{\omega}_d + k_s k_1 \omega_d \\ \frac{\partial u_f}{\partial t} &= \frac{\tau_d (\dot{\omega}_d + k_1 \omega_d) + \frac{\partial \tau_d}{\partial t} r}{B_2 \delta_d^2}, & \frac{\partial u_f}{\partial \hat{M}_m} &= \frac{\frac{\partial \tau_d}{\partial \hat{M}_m} r}{B_2 \delta_d^2} \end{aligned}$$

$$\begin{aligned} \frac{\partial u_f}{\partial \hat{\theta}_m} &= \frac{\frac{\partial \tau_d}{\partial \hat{\theta}_m} r}{B_2 \delta_d^2}, & \frac{\partial u_f}{\partial q} &= \frac{-\tau_d k_1 + \frac{\partial \tau_d}{\partial q} r}{B_2 \delta_d^2}, & \frac{\partial u_f}{\partial \omega} &= \frac{-\tau_d + \frac{\partial \tau_d}{\partial \omega} r}{B_2 \delta_d^2} \\ \frac{\partial u_f}{\partial \delta_d} &= -\left(\frac{\dot{\delta}_d}{B_2 \delta_d^2} + \frac{2\tau_d r}{B_2 \delta_d^3} \right), & \frac{\partial u_f}{\partial \dot{\delta}_d} &= \frac{1}{B_2 \delta_d}. \end{aligned}$$

APPENDIX II

The measurable auxiliary functions, $\Omega_a(t), \Omega_b(t) \in \mathbb{R}^2$, $\Omega_c(t), \Omega_d(t) \in \mathbb{R}^{2 \times 2}$ and $Y(t) \in \mathbb{R}^{2 \times p}$ used in the formulation of the stator control voltage inputs are listed below

$$\Omega_a = L_l \alpha_1 I^T J \psi_d \left[\frac{1}{\alpha_1 \delta_d^2} \frac{\partial \tau_d}{\partial \omega} J \psi_d + \frac{\partial u_f}{\partial \omega} \psi_d \right]$$

$$\begin{aligned} \Omega_b &= \frac{L_l}{\alpha_1 \delta_d^2} \left(\frac{\partial \tau_d}{\partial t} + \frac{\partial \tau_d}{\partial \hat{M}_m} \dot{M}_m + \frac{\partial \tau_d}{\partial q} \omega + \frac{\partial \tau_d}{\partial \hat{\theta}_m} \dot{\theta}_m \right) J \psi_d \\ &+ \frac{L_l \tau_d}{\alpha_1 \delta_d^2} J \psi_d - \frac{2L_l \tau_d \dot{\delta}_d}{\alpha_1 \delta_d^3} J \psi_d + L_l \left(\frac{\partial u_f}{\partial \delta_d} \dot{\delta}_d + \frac{\partial u_f}{\partial \dot{\delta}_d} \ddot{\delta}_d \right) \psi_d \\ &+ L_l \left(\frac{\partial u_f}{\partial t} + \frac{\partial u_f}{\partial \hat{M}_m} \dot{M}_m + \frac{\partial u_f}{\partial \hat{\theta}_m} \dot{\theta}_m + \frac{\partial u_f}{\partial q} \omega \right) \psi_d \\ &+ L_l u_f \psi_d - B_3 \psi_d + (R_l + L_l \omega J) I + \alpha_1 \omega J \psi_d \\ \Omega_c &= -\frac{L_l}{\delta_d^2} \frac{\partial \tau_d}{\partial \omega} J \psi_d I^T J - \alpha_1 L_l \frac{\partial u_f}{\partial \omega} \psi_d I^T J \\ \Omega_d &= -\alpha_1 \omega J \\ Y &= L_l \left(-\frac{1}{\alpha_1 \delta_d^2} \frac{\partial \tau_d}{\partial \omega} J \psi_d - \frac{\partial u_f}{\partial \omega} \psi_d \right) W_m(\omega). \end{aligned}$$

REFERENCES

- [1] F. Blaschke, "The principle of field orientation applied to the new transvector closed-loop control system for rotating field machines," *Siemens-Rev.*, vol. 39, pp 217-220, 1972.
- [2] W. Leonhard, "Microcomputer control of high dynamic performance ac drives – a survey," *Automatica*, vol. 22, pp. 1-19, 1986.
- [3] *Field Orientated Control of 3-Phase AC-Motors*, Texas Instruments Inc., Europe, 1998.
- [4] Z. Krzeminski, "Nonlinear control of induction motors," *Proc. 10th IFAC World Congress*, Munich, Germany, 1987, pp. 349-354.
- [5] S. S. Sastry and A. Isidori, "Adaptive control of linearizable systems," *IEEE Trans. Automat. Contr.*, vol. 34, pp. 1123-1131, 1989.
- [6] R. Marino, S. Peresada, and P. Valigi, "Adaptive input-output linearizing control of induction motors," *IEEE Trans. Automat. Contr.*, vol. 38, no. 2, pp. 208-221, Feb. 1993.
- [7] I. Kanellakopoulos, P. Krein, and F. Disivestro, "A new controller observer design for induction motor control," *Proc. ASME Winter Meeting*, Anaheim, CA, 1992, pp. 43-47.
- [8] I. Kanellakopoulos, and P. Krein, "Integral-action nonlinear control of induction motors," *Proc. 12th IFAC World Congress*, Sydney, Australia, 1993, pp. 1700-1704.
- [9] R. Canudas de Wit, R. Ortega and S. Seleme, "Robot motion control using induction motor drives," *Proc. IEEE International Conf. on Robotics and Automation*, Atlanta, GA, 1993, pp. 143-153.
- [10] J. Hu, D. Dawson, and Y. Qian, "Tracking control of robot manipulators driven by induction motors without flux measurements," *Proc. ASME Winter Meeting*, New Orleans, LA, 1993, pp. 43-47.
- [11] "—", "Position tracking control of an induction motor via partial state feedback," *Automatica*, vol. 31, pp. 989-1000, 1995.
- [12] G. Espinosa-Perez and R. Ortega, "State observers are necessary for induction motor control," *Syst. Control Lett.*, vol. 23, pp. 315-323, 1994

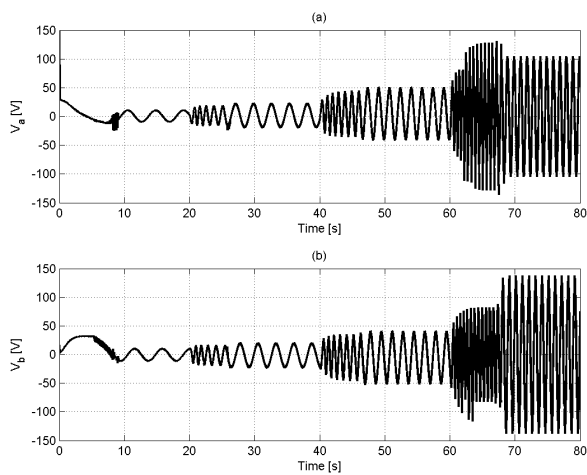


Fig. 8. Time evolution of the control voltage: (a) $V_a(t)$ and (b) $V_b(t)$ for nonlinear load case

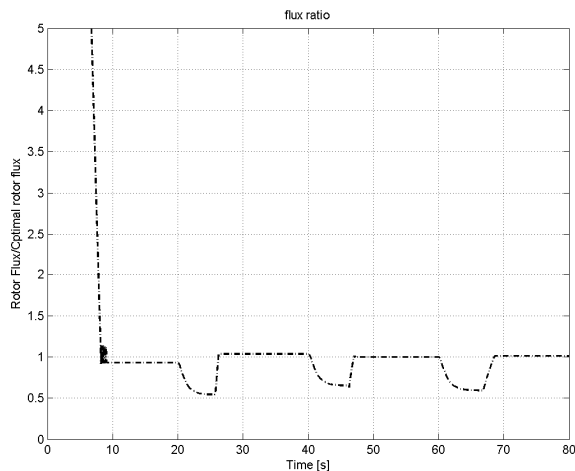


Fig. 9. The time evolution of the rotor magnitude ratio $\frac{\delta_d(t)}{\delta_d^*}$ for the nonlinear load case

[13] R. Ortega, P. Nicklasson, and G. Espinosa-Perez, "On speed control of induction motors," *Proc. American Control Conf.*, Seattle, WA, 1992, pp. 3521-3525.

[14] D. Dawson, J. Hu, and P. Vedagarbha, "An adaptive controller for a class of induction motor systems," *Proc. 33rd IEEE Conf. on Decision and Control*, Lake Buena Vista, FL, 1994, pp. 1567-1572.

[15] Y. Kim, S. Sul, and M. Park, "Speed sensorless vector control of induction motor using extended Kalman filter," *IEEE Trans. Ind. Appl.*, vol. 30, pp. 1225-1233, Sept. 1994.

[16] F. Peng and T. Fukao, "Robust speed identification for speed-sensorless vector control of induction motors," *IEEE Trans. Ind. Appl.*, vol. 30, pp. 1234-1240, Sept. 1994.

[17] J. Zamora, A. Garcia-Cerrada, and A. Zazo, "Rotor-speed estimator induction motors using voltage and current measurements," *IFAC J. Contr. Eng. Practice*, vol. 6, no. 3, pp. 369-383, Mar. 1998.

[18] R. Chang and F. Li-Chen, "Nonlinear adaptive sensorless speed control of induction motors," *Proc. 37th IEEE Conf. on Decision and Control*, Tampa, FL, 1998, pp. 965-970.

[19] M. Feemster, P. Aquino, D.M. Dawson, and A. Behal, "Sensorless rotor velocity tracking control for induction motors," *IEEE Trans. Contr. Syst. Tech.*, vol. 9, no. 4, pp. 645-653, July 2001.

[20] R. Marino, S. Peresada, and P. Valigi, "Exponentially convergent rotor resistance estimation for induction motors," *IEEE Trans. Ind. Electron.*, vol. 42, no. 5, pp. 508-515, July 1995.

[21] R. Soto and K. Yeung, "Sliding-mode control of an induction motor without flux measurements," *IEEE Trans. Ind. Appl.*, vol. 31, no. 4, pp. 744-750, 1995.

[22] C.M. Kwan, F.L. Lewis, and K.S. Yeung, "Robust adaptive control of induction motors without flux measurements," *Automatica*, vol. 32, pp. 903-908, 1996.

[23] R. Marino, S. Peresada, and P. Tomei, "Global adaptive output feedback control of induction motors with uncertain rotor resistance," *Proc. 35th Conf. on Decision and Control*, Kobe, Japan, 1996, pp. 4701-4706.

[24] J. Hu and D.M. Dawson, "Adaptive control of induction motor systems despite rotor resistance uncertainty," *Automatica*, vol. 32, pp. 1127-1143, 1996.

[25] P. Vedagarbha, M. Feemster, P. Aquino, and D.M. Dawson, "Non-linear adaptive control of induction motors," *Int. J. Adapt. Control Signal Processing*, vol. 13, pp. 367-392, 1999.

[26] D.S. Kirschen, D.W. Novotny and T.A. Lopo, "Optimal efficiency control of an induction motor drive," *IEEE Trans. Energy Conversion*, vol. 2, pp. 70-76, 1987.

[27] G. C. D. Sousa, B. K. Bose, and J. G. Cleland, "Fuzzy logic based on-line efficiency optimization control of an indirect vector-controlled induction motor drive," *IEEE Trans. Ind. Electron.*, vol. 42, no. 2, pp. 192-198, April 1995.

[28] I. Kioskeridis and N. Margaris, "Loss Minimization in scalar-controlled induction motor drives with search controllers," *IEEE Trans. Power Electron.*, vol. 11, no. 2, pp. 213-220, March 1996.

[29] E. Poirier, M. Ghribi, A. Kaddouri, "Loss minimization control of induction motor drives based on genetic algorithms", *IEEE International Electric Machines and Drives Conference IEMDC'01*, pp. 475-478, 2001.

[30] E. S. Abdin, G. A. Ghoneem, H. M. M. Diab, and S. A. Deraz, "Efficiency optimization of a vector controlled induction motor drive using an artificial neural network," *Proc. 29th Int. Conf. on Industrial Electron., Contr. and Instr.*, vol. 3, pp. 110-115, 2003.

[31] A.H.M Yatim and W.M. Utomo, "Efficiency Optimization of Variable Speed Induction Motor Drive Using Online Backpropagation," *IEEE Int. Power and Energy Conf.*, pp. 441-446, Nov. 2006 .

[32] J. Wu, D. Gao, X. Zhao, and Q. Lu, "An efficiency optimization strategy of induction motors for electric vehicles," *IEEE Vehicle Power and Propulsion Conference*, pp. 1-5, Sept. 2008.

[33] P. Vedagarbha, D.M. Dawson, and T. Burg "Rotor velocity/flux tracking control of induction motors with improved efficiency," *Mechatronics*, vol. 7, no. 2, pp. 105-127, 1997.

[34] P. Krause, O. Wasynczuk, and S. Sudhoff, *Analysis of Electric Machinery*. New York, NY: IEEE Press, 1994.

[35] D. Dawson, J. Hu, and T. Burg, *Nonlinear Control of Electric Machinery*. New York, NY: Marcel Dekker, 1998.

[36] P. A. Ioannou and J. Sun, *Robust Adaptive Control*. Upper Saddle River, NJ: Prentice Hall, 1996.

[37] M. Krstic, I. Kanellakopoulos and P. Kokotovic, *Nonlinear and Adaptive Control Design*. New York, NY: Wiley, 1995.

[38] W Dixon, A. Behal, D. Dawson, and S. Nagarkatti, *Nonlinear control of engineering systems: A Lyapunov-based approach*. Boston, MA: Birkhäuser, 2003.

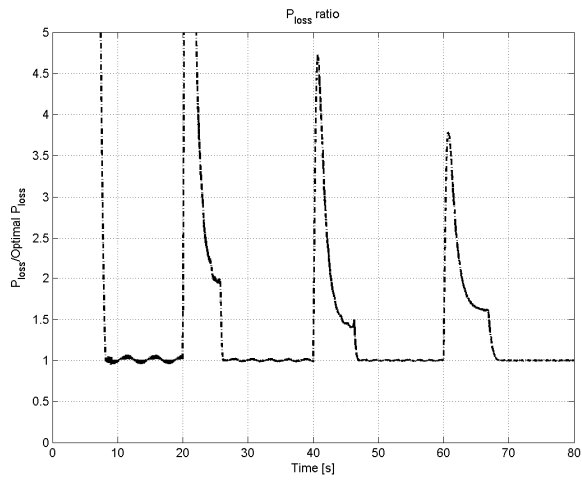


Fig. 10. The time evolution of the copper loss ratio $\frac{P_{loss}(t)}{P_{loss}^*}$ for the nonlinear load case